Synthesis, Characterization, and Mass Transport Properties of a Self-Generating Single-Source Magnesium Precursor for MOCVD of MgF_2 Films

Maria E. Fragalà,[†] Roberta G. Toro,[‡] Patrizia Rossi,[§] Paolo Dapporto,[§] and Graziella Malandrino*,[†]

Dipartimento di Scienze Chimiche, Università di Catania, and INSTM, UdR Viale Andrea Doria 6, 95125 Catania, Italy, INSTM, Centro di Riferimento "Materiali nanodimensionati per microelettronica e settori correlati", c/o Dipartimento Scienze Chimiche, Università di Catania, Viale A. Doria 6, 95125 Catania, Italy, and Dipartimento di Energetica "S. Stecco", Università di Firenze, Via Santa Marta 3, 50136 Firenze, Italy

Received October 26, 2008. Revised Manuscript Received March 26, 2009

The diglyme $[CH_3O(CH_2CH_2O)_2CH_3]$ adduct of the magnesium bis-hexafluoroacetyl-acetonato $[Mg(hfa)_2 \cdot 2H_2O \cdot 2diglyme]$ has been synthesized in a single-step reaction. It has been characterized by elemental analyses, IR spectroscopy, and ^1H and ^{13}C NMR. Single-crystal X-ray diffraction studies provide evidence of a mononuclear hexa-coordinated complex with an octahedral structure for the $Mg(hfa)_2 \cdot 2H_2O$ moiety and diglyme coordinated in the outer sphere (triclinic system, space group= $P\bar{1}$; $a = 8.952(3)$ Å, $b = 9.036(3)$ Å, $c = 11.98(1)$ Å, $\alpha = 110.44(5)°$, $\beta = 108.64(4)°$, $\gamma = 97.06(3)°$, $Z = 1$). The "thermal robustness" and mass transport properties of the adduct have been investigated by thermogravimetric analysis and chemical vapor deposition experiments. Thermal analysis data revealed high volatility and good thermal stability with a residue left lower than 1%. The $Mg(hfa)_2 \cdot 2H_2O \cdot 2diglyme$ has been successfully applied to the low-pressure metal-organic chemical vapor deposition (MOCVD) of MgF_2 films. The good quality of the deposited films indicates that the adduct is a very attractive single-source precursor for deposition of MgF_2 films.

Introduction

Magnesium fluoride represents a really interesting material widely used in both the infrared and ultraviolet because of the useful transmission range from 0.11 to 7.5 μm.[1] Interesting enough, it is the only optical material that combines a wide spectral transmittance band with birefringence phenomena. MgF_2 is also a shock- and water-resistant material and, moreover, not susceptible to radiation-induced color centers. In terms of optical applications, MgF_2 is a proven material for high-energy lasers and, in particular, for application in both UV and vacuum ultraviolet (VUV) regions.[2] In this latter scenario, the extension of excimer lasers to extreme UV region has fueled the demand for low-loss optical components and metal fluorides are excellent candidates for such purposes.

MgF_2 is a wide band gap insulator and its low refractive index favors the combination with high refractive index materials (such as LaF_3, Al_2O_3, or TiO_2) for optical multilayers, high reflective mirrors, and narrow band-pass filters.[3] MgF_2 has been also extensively used as an antireflection coating material.[4]

Large parts of these applications[3,4] require MgF_2 in form of thin films. Several deposition routes have been presented and discussed in the literature. Physical vapor deposition techniques (PVD) seem to emerge from the scrutiny of data.[3,5] Chemical solution routes, such as sol−gel, have been applied to prepare MgF_2 films, but they are not commonly adopted because of difficulty in handling fluorine sources, usually hazardous HF or F_2 gas.[6]

Atomic layer deposition (ALD) has been successfully proposed in recent papers and, despite the good quality of

[†] Dipartimento di Scienze Chimiche, Università di Catania, and INSTM.
[‡] INSTM, Centro di Riferimento "Materiali nanodimensionati per microelettronica e settori correlati", c/o Dipartimento Scienze Chimiche, Università di Catania.
[§] Università di Firenze.

(1) (a) Belanger, D. P.; King, A. R.; Jaccarino, V. *Phys. Rev. B: Condens. Matter* **1984**, *29*, 2636. (b) Fukumoto, E.; Aoki, T.; Ogura, S. *Trends Opt. Photonics* **2001**, *63*, TuF9/1, Optical Interference Coatings. (c) Larruquert, J. I.; Keski-Kuha, R. A. M. *Opt. Commun.* **2003**, *215*, 93.
(2) Perales, F.; Herrero, J. M.; Jaque, D.; de las Heras, C. *Opt. Mater.* **2007**, *29*, 783.
(3) (a) Gunster, S.; Kadkhoda, P.; Ristau, D. *Trends Opt. Photonics* **2001**, *63*, ME9/1, Optical Interference Coatings. (b) Li, B.; Martin, S.; Welsch, E. *Appl. Phys. A: Mater. Sci. Process.* **2002**, *74*, 27. (c) Czigany, Zs.; Adamik, M.; Kaiser, N. *Thin Solid Films* **1998**, *312*, 176. (d) Woo, S.-H.; Hwangbo, C. K. *Surf. Coat. Technol.* **2007**, *201*, 8250.
(4) Thomas, I. M. *Appl. Opt.* **1988**, *27*, 3356.
(5) Jacob, D.; Peiro, F.; Quesnel, E.; Ristau, D. *Thin Solid Films* **2000**, *360*, 133.
(6) (a) Murata, T.; Ishizawa, H.; Tanaka, A. *Appl. Opt.* **2008**, *47*, C246. (b) Krueger, H.; Kemnitz, E.; Hertwig, A.; Beck, U. *Thin Solid Films* **2008**, *516*, 4175. (c) Bass, J. D.; Boissiere, C.; Nicole, L.; Grosso, D.; Sanchez, C. *Chem. Mater.* **2008**, *20*, 5550. (d) Rywak, A. A.; Burlitch, J. M. *Chem. Mater.* **1996**, *8*, 60.
(7) (a) Pilvi, T.; Puukilainen, E.; Kreissig, U.; Leskela, M.; Ritala, M. *Chem. Mater.* **2008**, *20*, 5023. (b) Pilvi, T.; Hatanpaeae, T.; Puukilainen, E.; Arstila, K.; Bischoff, M.; Kaiser, U.; Kaiser, N.; Leskela, M.; Ritala, M. *J. Mater. Chem.* **2007**, *17*, 5077. (c) Pilvi, T.; Ritala, M.; Leskela, M.; Bischoff, M.; Kaiser, U.; Kaiser, N. *Appl. Opt.* **2008**, *47*, C271.

10.1021/cm802923w CCC: $40.75
Published on Web 04/23/2009

the obtained film, the procedure requires specific F sources (namely, TiF_4 or TaF_5) that are expensive and require careful handling.[7] In summary, this contribution reports the use of an easily synthesized magnesium adduct as a clean single-source Mg/F precursor for the deposition of crystalline MgF_2 thin films under very mild MOCVD conditions. To the best of our knowledge, neither chemical vapor deposition (CVD)[8] or metal-organic CVD processes have been adopted for the deposition of MgF_2 films. On the other hand, there is a wide literature on the MOCVD of MgO films.[9] Various thermally stable and volatile precursors have been reported, but most of them are fluorine-free; therefore, their applications to the growth of MgF_2 films would require the use of hazardous fluorine sources.[10]

Moreover, Mg is also considered an effective dopant element for the ceria-based electrolytes[11] and the $LaGaO_3$- and $LaCrO_3$-based electrodes[12] in solid oxide fuel cells (SOFC).

In early papers, we have discussed the favorable properties of a large family of single-source precursors to fabricate high-quality films of alkaline-[13] and rare-earth fluorides.[14] These sources are based on molecular architectures consisting of a fluorinated β-diketonate metal array whose coordinative deficiency was saturated by various Lewis base ligands, such as polyglymes.[15]

The ancillary polyglyme coordination was proved to strongly stabilize the metal center and to preclude oligomerization, thus resulting in monomeric, thermally stable, highly volatile, and low melting adducts. All these properties are of relevance and, in particular, liquid or low melting precursors represent the most desirable sources because of the greater and stable vapor pressure, the absence of any effects of crystallite size on the evaporation rate, and hence, on the film growth rate. Solid precursors suffer from unstable vapor pressures in the reactor during the film growth. In fact, note that the crystallite size may be responsible for changes in evaporation rates in different runs and, even more important, in variations during the same experiment.[16]

In this general perspective, we focused our research on the synthesis of a second-generation magnesium single-source precursor, suited for the fabrication of MgF_2 thin films.

Herein, we report the synthesis and transport characteristics of a new magnesium precursor of formula $Mg(hfa)_2 \cdot 2H_2O \cdot$ 2diglyme [Hhfa = 1,1,1,5,5,5-hexafluoro-2,4-pentanedione and diglyme = (bis(2-methoxyethyl)ether)], and discuss the thermal stability and volatility compared to the parent $Mg(hfa)_2 \cdot 2H_2O$ complex. It will be shown that the $Mg(hfa)_2 \cdot 2H_2O \cdot$2diglyme represents a suited single-source precursor for the growth of pure magnesium fluoride thin films by MOCVD on glass and quartz substrates.

Experimental Section

Reagents. Commercial $(MgCO_3)_4 \cdot Mg(OH)_2 \cdot 5H_2O$, Hhfa, diglyme were purchased from Sigma-Aldrich and used without any further purification.

General Procedures. Elemental microanalyses were performed in the Analytical Laboratories of the University of Catania. Infrared transmittance spectra were recorded using a Jasco FT/IR-430 spectrometer as nujol mulls between NaCl plates. The instrumental resolution was 2 cm^{-1}. ^1H and ^{13}C NMR spectra were recorded on a Varian Inova 500 spectrometer.

Thermal measurements were made using a Mettler Toledo TGA/SDTA 851^e, a TC 10 processor and DSC 30 calorimeter. Dynamic thermal investigations were carried out under purified nitrogen flow (30 sccm) at atmospheric pressure using a 5 °C/min heating rate. Weights of the samples were between 15−20 mg (TGA) and 4−10 mg (DSC). The temperature was measured with an accuracy of ±0.1 °C. Isothermal investigations were carried out at 20 Torr, using a 5 °C/min heating rate to reach the set point temperature. It thus takes from 7 min (for the isothermal curve carried out at 60 °C starting from RT = 25 °C) to 17 min for the highest temperature of 110 °C. Nitrogen has been used as buffer gas flow with a flow rate of 30 sccm. The cylindrical sample boat (12.56 mm^2 cross-sectional area) was filled with ∼15 mg of the magnesium adduct and placed on a sample holder in a horizontal tube furnace. The melting points were measured in air with a Koffler microscope.

Synthesis of $Mg(hfa)_2 \cdot 2H_2O \cdot$2diglyme (1). $(MgCO_3)_4 \cdot Mg(OH)_2 \cdot 5H_2O$ (2.043 g, 4.21 mmol) was first suspended in dichloromethane (15 mL). Diglyme (0.943 g, 7.0 mmol) was added to the suspension. Hhfa (2.94 g, 14.0 mmol) was added under vigorous stirring after 10 min and the mixture was refluxed under stirring for 1 h. The excess of Mg basic carbonate was filtered off. Colorless crystals precipitated after partial evaporation of the solvent. The crystals were collected, washed with pentane, filtered, and dried under a vacuum. The yield was 86%. The melting point of the crude product was 48−50 °C. Anal. Calcd (Found) for $MgC_{22}H_{34}F_{12}O_{12}$: C, 35.59 (34.93); H, 4.61 (4.24). The adduct quantitatively sublimes at 55−60 °C/10^{-2} mmHg. IR (nujol; ν, cm^{-1}): 3475 (w), 3290 (w), 2923 (vs), 1660 (vs), 1619 (w), 1599 (w), 1558 (m), 1534 (s), 1512 (s), 1462 (s), 1455 (vs), 1380 (m), 1350 (w), 1260 (s), 1217 (s), 1190 (w), 1148 (m), 1100 (m), 1015 (vw), 942 (w), 862 (m), 838 (m), 800 (m), 770 (w), 740 (w), 667 (s). ^1H NMR ($CDCl_3$): δ 6.06

(8) Hitchman, M. L.; Jensen, K. F.; *Chemical Vapor Deposition: Principles and Applications*; Academic Press: London, 1993.
(9) (a) Wang, L.; Yang, Y.; Ni, J.; Stern, C. L.; Marks, T. J. *Chem. Mater.* **2005**, *17*, 5697. (b) Carta, G.; El Habra, N.; Crociani, L.; Rossetto, G.; Zanella, P.; Zanella, A.; Paolucci, G.; Barreca, D.; Tondello, E. *Chem. Vap. Deposition* **2007**, *13*, 185. (c) Boo, J.-H.; Lee, S.-B.; Yu, K.-S.; Koh, W.; Kim, Y. *Thin Solid Films* **1999**, *341*, 63. (d) Matthews, J. S.; Just, O.; Obi-Johnson, B.; Rees, W. S., Jr. *Chem. Vap. Deposition* **2000**, *6*, 129.
(10) (a) Hill, M. R.; Jones, A. W.; Russell, J. J.; Roberts, N. K.; Lamb, R. N. *J. Mater. Chem.* **2004**, *14*, 3198. (b) Davies, H. O.; Jones, A. C.; Leedham, T. J.; Crosbie, M. J.; Wright, P. J.; Boag, N. M.; Thompson, J. R. *Chem. Vap. Deposition* **2000**, *6*, 71. (c) Hatanpaa, T.; Kansikas, J.; Mutikainen, I.; Leskela, M. *Inorg. Chem.* **2001**, *40*, 788.
(11) Zheng, Y.; Gu, H.; Chen, H.; Gao, L.; Zhu, X.; Guo, L. *Mater. Res. Bull.* **2009**, *44*, 775.
(12) (a) Datta, P.; Bronin, D. I.; Majewski, P.; Aldinger, F. *Mater. Chem. Phys.* **2009**, *114*, 356. (b) Ghosh, S.; Das Sharma, A.; Basu, R. N.; Maiti, H. S. *J. Am. Ceram. Soc.* **2007**, *90*, 3741.
(13) Malandrino, G.; Castelli, F.; Fragalà, I. L. *Inorg. Chim. Acta* **1994**, *224*, 203.
(14) (a) Malandrino, G.; Perdicaro, L. M. S.; Fragalà, I. L. *Chem. Vap. Deposition* **2006**, *12*, 736. (b) Lo Nigro, R.; Toro, R.; Malandrino, G.; Fragalà, I. L.; Rossi, P.; Dapporto, P. *J. Electrochem. Soc.* **2004**, *151*, F206. (c) Lo Nigro, R.; Malandrino, G.; Fragalà, I. L.; Bettinelli, M.; Speghini, A. *J. Mater. Chem.* **2002**, *12*, 2816. (d) Malandrino, G.; Benelli, C.; Castelli, F.; Fragalà, I. L. *Chem. Mater.* **1998**, *10*, 3434. (e) Malandrino, G.; Fragalà, I. L.; Aime, S.; Dastrù, W.; Gobetto, R.; Benelli, C. *J. Chem. Soc., Dalton Trans.* **1998**, 1509. (f) Malandrino, G.; Incontro, O.; Castelli, F.; Fragalà, I. L.; Benelli, C. *Chem. Mater.* **1996**, *8*, 1292.
(15) Malandrino, G.; Fragalà, I. L. *Coord. Chem. Rev.* **2006**, *250*, 1605, and references therein.
(16) Hitchman, M. L.; Shamlian, S. H.; Gilliland, D. C.; Cole-Hamilton, D.; Nash, J. A. P.; Thompson, S. C.; Cook, S. L. *J. Mater. Chem.* **1995**, *5*, 47.

(s, 2H); 3.6−3.7 (m, 8H); 3.40 (s, 6H); 2.2−2.3 (s, 4H). ^{13}C NMR (CD_3CN): δ 58.13 (s, OCH_3); 70.19 (s, OCH_2); 71.85 (s, OCH_2); 88.99 (s, *C*H); 117 (q, *C*F_3, ^1J = 284 Hz); 176 (q, *C*O, ^2J = 33 Hz).

Synthesis of Mg(hfa)$_2$·2H$_2$O (2). Prepared using a procedure analogous to that described for the diglyme adduct (**1**) from 2.072 g (4.27 mmol) of $(MgCO_3)_4$·$Mg(OH)_2$·$5H_2O$, 4.41 g (21.30 mmol) of Hhfa. Yield 81%. The compound melts at 200−203 °C. Anal. Calcd (Found) for $MgC_{10}H_6F_{12}O_6$: C 25.31 (24.59), H 1.27 (1.39) %. IR (nujol;ν, cm^{-1}): 3506 (s), 3413 (s), 2923 (s), 1657 (s), 1605 (w), 1565 (m), 1530 (m), 1495 (s), 1460 (s), 1376 (m), 1350 (vw), 1260 (s), 1251 (s), 1231(s), 1205 (s), 1145 (s), 1098 (w), 807 (m), 770 (vw), 740 (w), 669 (s). ^{1}H NMR (CD_3COCD_3): δ 5.97 (s, 2H); 3.5 (s, 4H).

X-ray Structural Determination of Mg(hfa)$_2$·2H$_2$O·2diglyme (1). X-ray grade single crystal of Mg(hfa)$_2$·2H$_2$O·2diglyme was grown from hexane. Cell parameters and intensity data for Mg(hfa)$_2$·2H$_2$O·2diglyme were obtained on a Nonius Mach3 diffractometer, using graphite monochromathed Mo Kα radiation (λ = 0.71069 Å). Cell parameters were determined by least-squares fitting of 25 centered reflections. The intensities of two standard reflections were measured every 60 min to check the stability of the diffractometer and the decay of the crystal. Intensity data were corrected for Lorentz and polarization effects, an absorption correction was applied once the structure was solved by using the Walker and Stuart method.[17] The structure was solved using the SIR-97[18] program and subsequently refined by the full-matrix least-squares program SHELX-97.[19] All the hydrogen atoms of the diglyme molecule and of the hfa anion were found in the Fourier difference map and refined isotropically. All the non-hydrogen atoms were refined anisotropically. Fluorine atoms have, as expected, rather large anisotropic factors. Atomic scattering factors and anomalous dispersion corrections for all the atoms were taken from ref 20. Geometrical calculations were performed by PARST97.[21] The molecular plot was produced by the ORTEP-3 program.[22] Crystal and structure refinement data are reported in Table 1. Table 2 reports bond lengths (Å) and angles (deg) for Mg(hfa)$_2$·2H$_2$O·2diglyme.

MOCVD Experiments and Film Characterization. MOCVD depositions of MgF_2 films were performed using a horizontal hot-wall reactor from the Mg(hfa)$_2$·2H$_2$O·2diglyme (**1**) source. Deposition temperatures were settled in the 350−650 °C range. Glass or quartz substrates were used for the deposition. The source temperature was controlled in the 70−100 °C range. Ar (100 sccm) and O_2 (100 sccm) flows were used as carrier and reaction gases, respectively. The mass flows were controlled with 1160 MKS flowmeter using an MKS 147 electronic control unit. Depositions were carried out for 60 min. The total pressure in the reactor was about 2 Torr.

$\theta-2\theta$ X-ray diffraction (XRD) patterns were recorded on a Bruker-AXS D5005 $\theta-\theta$ X-ray diffractometer, using a Cu Kα radiation operating at 40 kV and 30 mA and a step of 0.05°. Film surface morphology was examined using a LEO Iridium 1450 scanning electron microscope (SEM). Film atomic composition was determined by energy dispersive X-ray analysis (EDX), using an IXRF detector, and by X-ray photoelectron analysis (XPS) using a PHI ESCA/SAM 5600 Multy technique spectrometer. XPS experiments were carried out with a base pressure of 2×10^{-10} Torr. A standard Al Kα radiation source ($h\nu$ = 1486.6 eV) was used and XPS spectra were collected at a photoelectron angle of 45°.

Table 1. Crystal Data and Structure Refinement for Mg(hfa)$_2$·2H$_2$O·2diglyme

empirical formula	$C_{22}H_{34}F_{12}Mg_1O_{12}$
fw	742.8
T (K)	200
λ (Å)	0.71069
cryst syst, space group	triclinic, $P\bar{1}$
a (Å)	8.952(3)
b (Å)	9.036(3)
c (Å)	11.98(1)
α (deg)	110.44(5)
β (deg)	108.64(4)
γ (deg)	97.06(3)
V (Å^3)	829.9(8)
Z, d_{calcd} (g/cm^3)	1, 1.486
absorp coeff (mm^{-1})	0.174
no. of reflns collected/unique	3061/2911 [R(int) = 0.0174]
data/params	2911/284
final R indices [$I > 2\sigma(I)$]	R_1 = 0.0773, wR_2 = 0.2212
R indices (all data)	R_1 = 0.0880, wR_2 = 0.2338

Table 2. Bond lengths (Å) and Angles (deg) of Mg(hfa)$_2$·2H$_2$O·2diglyme[a]

Mg(1)−O(1)	2.073(3)
Mg(1)−O(2)	2.065(3)
Mg(1)−O(1w)	2.051(3)
O(1)−Mg(1)−O(2)	92.7(1)
O(1)−Mg(1)−O(1w)	91.5(1)
O(2)−Mg(1)−O(1w)	89.7(1)
O(1)−Mg(1)−O(2)′	92.8(1)
O(1)−Mg(1)−O(1w)′	88.4(1)
O(2)−Mg(1)−O(1w)′	89.7(1)

Intermolecular Hydrogen Bonds

	O···O distance	OH distance	O−H···O angle
O(1w)−H(1w)···O(3)	2.765(3)	1.96(6)	175(5)
O(1w)−H(2w)···O(5)	2.754(3)	2.00(6)	171(7)

[a] Symmetry transformation: ′ = $-x+1, -y, -z+1$.

Results and Discussion

Synthesis. The Mg(hfa)$_2$·2H$_2$O·2diglyme adduct has been prepared through a one-pot reaction from the magnesium basic carbonate source, hexafluoroacetylacetone and diglyme in dichloromethane (eq 1)

$$(MgCO_3)_4{\cdot}Mg(OH)_2{\cdot}5H_2O + 10\text{Hhfa} + 10\ \text{diglyme} \rightarrow 5\text{Mg(hfa)}_2{\cdot}2H_2O{\cdot}2\text{diglyme} + H_2O + 4CO_2 \quad (1)$$

The procedure yields reproducibly, under open bench manipulations, a clean source adduct. A slight excess of Mg carbonate favors the isolation of the product since the excess remains insoluble and can be easily filtered off. The adduct is very soluble in common organic solvents such as ethanol, chloroform, acetone, and pentane and slightly soluble in cyclohexane. It has a very low melting point and evaporates quantitatively at low temperature under vacuum and even under atmospheric pressure despite the presence of coordinated water.

In fact, the synthesis, carried out in dichloromethane with good yields, gives rise to adduct (**1**) having two H_2O molecules coordinated to the Mg center, and thus the diglyme cannot efficiently act as partitioning agent. Any attempt to

(17) Walker, N.; Stuart, D. D. *Acta Crystallogr., Sect. A,* **1983**, *39*, 158.
(18) Altomare, A.; Cascarano, G.; Giacovazzo, C.; Guagliardi, A.; Burla, M. C.; Polidori, G.; Camalli, M. *J. Appl. Crystallogr.* **1994**, *27*, 435.
(19) Sheldrick, G. M. *SHELXL-97*; University of Göttingen: Göttingen, Germany, 1997.
(20) *International Tables for X-ray Crystallography*; Kynoch Press: Birmingham, U.K., 1974; Vol. 4.
(21) Nardelli, M. *Comput. Chem.* **1993**, *7*, 95.
(22) Farrugia, L. J. *J. Appl. Crystallogr.* **1997**, *30*, 565.

Table 3. Correlation between Ionic Radii and Coordination Number for Alkaline Earth Metals[a]

metal ion	ionic radius (Å)	coordination number	ref
Mg(II)	0.65	6	this work
Ca(II)	0.99	8	25
Sr(II)	1.13	9	25
Ba(II)	1.35	9−10	23−25
Zn(II)	0.74	6	26b
Co(II)	0.74	6	26a

[a] Transition metals with ionic radii comparable to the Mg one are also reported.

produce the water-free adduct, even using a 1:2 Mg:diglyme ratio in the reaction mixture, proved unsuccessful. Oily products, whose nature prevented any further purification/crystallization, have always been obtained.

Note that, at variance with the present Mg adduct, many parent homologues of Ca, Sr, and Ba with longer glymes are water-free because of the larger ionic radii, which enables the glyme ligand to encapsulate the metal ion, thus preventing any water coordination.[13,23] This may be explained considering that the coordination sphere of any central metal ion crucially depends on the subtle interplay between the ionic radius and the ion charge. Namely, for a given charge, the larger the ion, the higher the coordination number. In the case of the alkaline earth metals, coordination numbers up to 11 have been observed in the case of the large Ba metal.[24,25] In Table 3, the ionic radii of the alkaline earth metals are summarized in relation to the most commonly observed coordination. For example, in the case of Ca, eight is the most common coordination number; for the $Ca(hfa)_2$·tetraglyme (where a maximum coordination number of 9 could have been reached), one oxygen of the tetraglyme is not coordinated.[25] Data related to Zn and Co transition metals are reported as well, because the diglyme and tetraglyme adducts of zinc and cobalt, respectively, present similar structures (vide infra), clearly due to the comparable value of ionic radii.[26]

The present findings reinforce our earlier assertion that the one-pot synthesis, already adopted for the preparation of alkaline-earth (M = Ba, Sr, and Ca)[13,24b] and rare-earth[14] metal adducts, is a "general-purpose" viable route, also applicable for Mg sources.

X-ray Single-Crystal Structures of the $Mg(hfa)_2·2H_2O·$ 2diglyme. The $Mg(hfa)_2·2H_2O·$2diglyme complex crystallizes in the triclinic space group $P\bar{1}$ with one unit in a cell of dimension $a = 8.952(3)$ Å, $b = 9.036(3)$ Å, $c = 11.98(1)$ Å, $\alpha = 110.44(5)°$, $\beta = 108.64(4)°$, and $\gamma = 97.06(3)°$. A view of the complex is given in Figure 1. Bond lengths and angles are reported in Table 2. The asymmetric unit of $Mg(hfa)_2·2H_2O·$2diglyme contains half of the magnesium

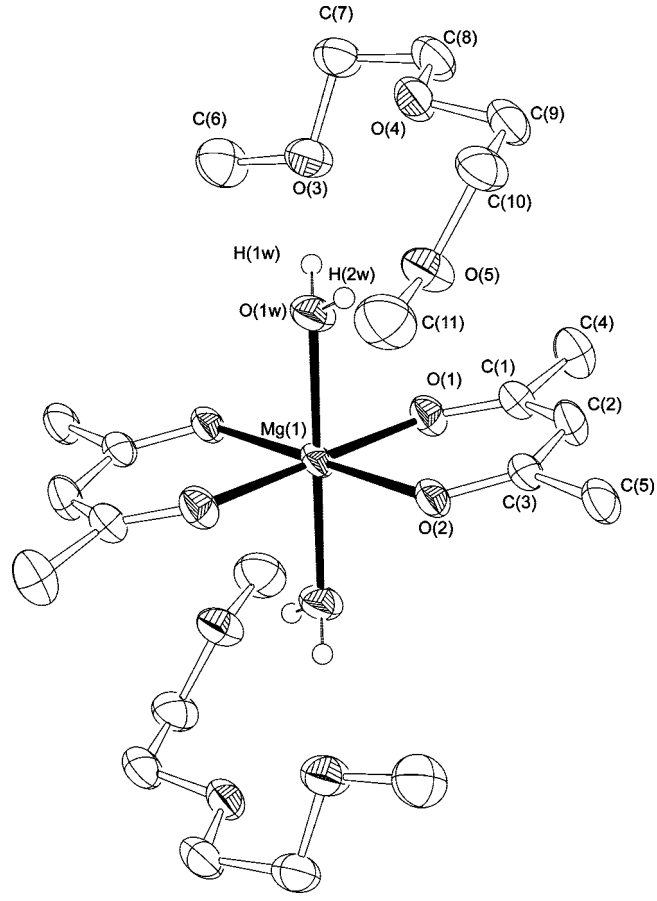

Figure 1. ORTEP3 view of $Mg(hfa)_2·2H_2O·$2diglyme. Fluorine and hydrogen atoms have been omitted for clarity.

complex $Mg(hfa)_2·2H_2O$ and one diglyme molecule. The two halves of the complex are related by a center of symmetry.

The magnesium cation Mg(1) (see Figure 1 for the atom labeling) is hexa-coordinated by four oxygen atoms of two hfa anions and by two oxygen atoms of the two water molecules. The octahedral co-ordination around the Mg atom is fairly regular. The $Mg-O_{hfa}$ distances are in agreement with those retrieved in the Cambridge Structural Database (CSD, v 5.29) for magnesium complexes of acetylacetonate derivatives.

Due to the presence of the center of symmetry the metal cation lies in the plane defined by O(1), O(2), O(1)′, and O(2)′. The angle between the line connecting the two oxygen atoms O(1w) and O(1w)′ (′ = $-x + 1, -y, -z + 1$) and the plane defined by the four oxygen atoms of the two hfa anions is 88.57(4)°.

The diglyme molecule does not coordinate the metal cation but interacts via hydrogen bonds with the coordinating water molecules. In fact, two short interactions are present in the asymmetric unit involving the oxygen atoms O(3) and O(5) and the water hydrogen atoms (see Figure 2 and Table 2). The conformation taken by the diglyme molecule is, as expected due to the presence of the strong hydrogen bonds, trans−gauche−trans−trans−gauche−trans.

The Cambridge Structural Database (v 5.29) was used to search complexes of general formula $M(hfa)_2·2H_2O$, where M is an hexa-coordinated metal cation. In all, 19 complexes were retrieved having an octahedron as coordination poly-

(23) (a) Timmer, K.; Spee, K. I. M. A.; Mackor, A.; Meinema, H. A.; Spek, A. L.; van der Sluis, P. *Inorg. Chim. Acta* **1991**, *190*, 109. (b) Malandrino, G.; Fragalà, I. L.; Neumayer, D. A.; Stern, C. L.; Hinds, B. J.; Marks, T. J. *J. Mater. Chem.* **1994**, *4*, 1061.
(24) (a) Neumayer, D. A.; Studebaker, D. B.; Hinds, B. J.; Stern, C. L.; Marks, T. J. *Chem. Mater.* **1994**, *6*, 878. (b) Belot, J. A.; Neumayer, D. A.; Reedy, C. J.; Studebaker, D. B.; Hinds, B. J.; Stern, C. L.; Marks, T. J. *Chem. Mater.* **1997**, *9*, 1638.
(25) Otaway, D. J.; Rees, W. S. *Coord. Chem. Rev.* **2000**, *210*, 279, and references therein.
(26) (a) Gulino, A.; Dapporto, P.; Rossi, P.; Fragalà, I. *Chem. Mater.* **2003**, *15*, 3748. (b) Gulino, A.; Castelli, F.; Dapporto, P.; Rossi, P.; Fragalà, I. *Chem. Mater.* **2000**, *12*, 548.

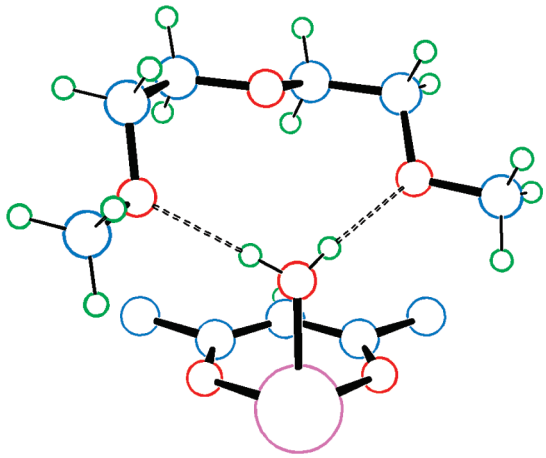

Figure 2. Scheme of the asymmetric unit of the $Mg(hfa)_2 \cdot 2H_2O \cdot 2diglyme$ complex evidencing the hydrogen bonds.

hedron; in particular, in 14 complexes, the water oxygen atoms form with the metal cation an angle of about 180°. Instead, the parent $Mg(hfa)_2 \cdot 2H_2O$ complex (CCDC refcode HOWGIJ) shows a distorted octahedral coordination geometry of the magnesium cation, but the water oxygen atoms are not in opposite position with respect to the metal cation (as in $Mg(hfa)_2 \cdot 2H_2O \cdot 2diglyme$) and form with it an angle of about 85°.[27] Two of the 19 complexes [CCDC refcodes AQIMUI (cobalt complex) and RAHVIF (zinc complex)] contain in their asymmetric unit a polyglyme molecule, tetraglyme, and diglyme for AQIMUI and RAHVIF, respectively.[26] In both cases, the water molecules are in opposite position with respect to the metal cation. As found in $Mg(hfa)_2 \cdot 2H_2O \cdot 2diglyme$, the polyglyme molecule does not coordinate the metal cation but two of its oxygen atoms interact via hydrogen bonds with a coordinating water molecule. The $O_{water} \cdots O_{hfa}$ distances are similar in all three structures, the main difference between them is that although in the zinc complex just one water molecule interacts with diglyme, in the $Mg(hfa)_2 \cdot 2H_2O \cdot 2diglyme$ complex the two water molecules form hydrogen bonds with two diglyme molecules. Finally, in the cobalt complex a tetraglyme molecule bridges together two complexes, giving rise to a chain.

Infrared Spectra. The FT-IR transmittance spectrum of the $Mg(hfa)_2 \cdot 2H_2O \cdot 2diglyme$ adduct (Figure 3a) shows a broad envelope with two bumps in the 3292 and 3487 cm^{-1} range due to the OH asymmetric and symmetric stretching modes of coordinated water.[26b] The carbonyl stretching frequency appears at 1657 cm^{-1}, whereas peaks at 1558 and 1534 cm^{-1} are associated with C═C stretching and with C═O stretching/C−H bending vibrations, respectively.[28] The broadband observed in the 1000−1300 cm^{-1} range may be associated with absorptions of the polyether C−O bending and/or stretching overlapped with the C−F stretching. In addition, bands at 1015, 861, and 837 cm^{-1} can be associated with glyme modes. The C−H glyme stretching modes, lying

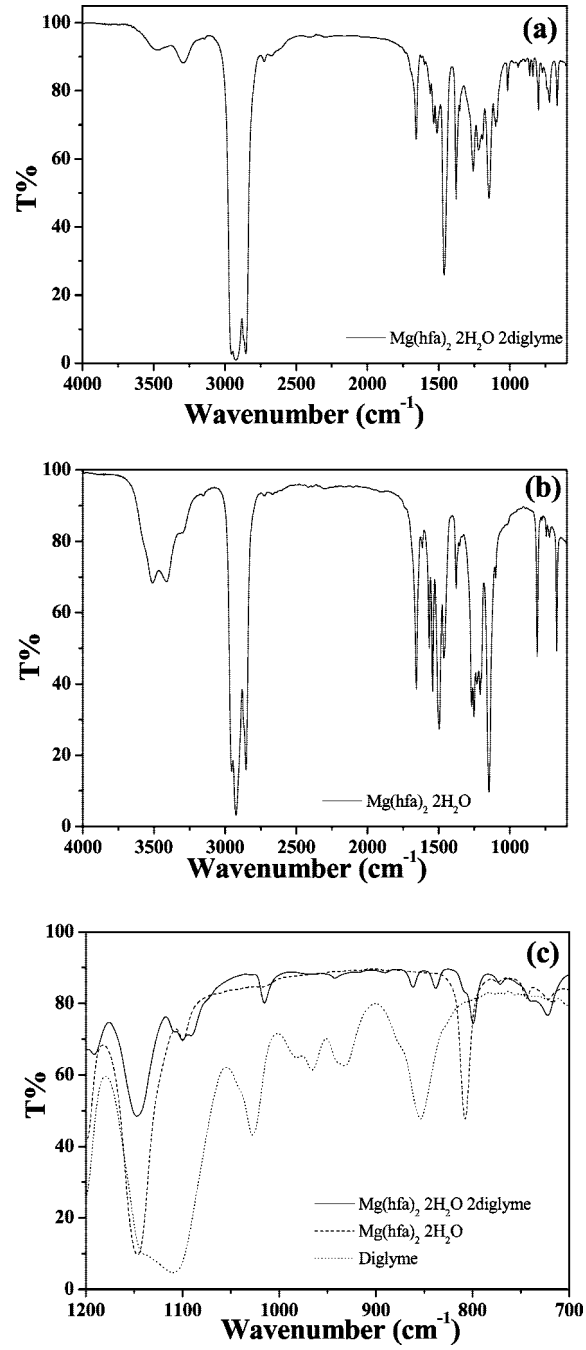

Figure 3. FT-IR spectra (nujol mulls) of (a) $Mg(hfa)_2 \cdot 2H_2O \cdot 2diglyme$,(b) $Mg(hfa)_2 \cdot 2H_2O$, and (c) a magnification of the fingerprint region for diglyme coordination (diglyme is reported as a neat sample).

in the 2800−3000 cm^{-1} range, overlap with nujol features. In fact, the nujol shows peaks at 2923, 1461, and 1377 cm^{-1}.

Analogously, the spectrum of the $Mg(hfa)_2 \cdot 2H_2O$ (Figure 3b) shows a broad envelope in the range 3300−3500 cm^{-1} range due to the coordinated water. Note that the shape of this band is much more complex and it is likely due to the presence of intermolecular hydrogen bonds among molecules.[27] The C═O stretching is similarly observed at 1653 cm^{-1}, whereas the C═C stretching and C═O stretching/C−H bending vibrations are associated with the absorptions at 1569 and 1541 cm^{-1}, respectively.

A magnification of the fingerprint region is reported in Figure 3c. Note that the peak at 854 cm^{-1} in adduct **1** is split, with respect to the free diglyme, in two peaks. This

(27) Kuz'mina, N. P.; Ryazanov, M. V.; Troyanov, S. I.; Martynenko, L. I.; Korsakov, I. E. *Russ. J. Coord.Chem.* **1999**, *25*, 383.
(28) (a) Condorelli, G. G.; Gennaro, S.; Fragalà, I. L. *Chem. Vap. Deposition* **2001**, *7*, 151. (b) Condorelli, G. G.; Gennaro, S.; Fragalà, I. L. *Chem. Vap. Deposition* **2000**, *6*, 185.

may be likely associated with the two different C−O stretchings for the diglyme oxygen atoms O3 and O5 (see Figure 2), which coordinate a H_2O molecule through hydrogen bonding and O4, which is uncoordinated.

NMR Spectra. The ^1H NMR ($CDCl_3$) and ^{13}C NMR (CD_3CN) spectra can be assigned using comparative arguments with data from closely related complexes.[13] The ^1H NMR spectrum of the $Mg(hfa)_2 \cdot 2H_2O \cdot 2$diglyme adduct shows a singlet at $\delta = 6.04-6.07$, whose integration accounts for the two protons of the hfa ring ligands. In addition, multiplets at $\delta = 3.6-3.7$ represent resonances of methylenic protons of the diglyme, whereas the singlet at $\delta \approx 3.40$ is consistent with the protons of the two methyl groups of the same ligand. Finally, the resonance at $\delta = 2.2-2.3$ (four protons) is associated with the two coordinated H_2O molecules.The ^{13}C NMR spectrum shows several resonances that can be assigned to hfa and diglyme ligand. Resonances associated with the coordinated hfa ligands consist, in all cases, of a singlet ($\delta = 88.99$) for the *C*H groups, a quartet ($\delta \approx 117$) for the *C*F_3 groups, and a quartet ($\delta \approx 176$) for the *C*O groups. The quartets are due to first-order (CF_3; $^1J = 284$ Hz) and second-order (CO; $^2J = 33$ Hz) coupling with the CF_3 fluorine atoms. Coordinated diglyme give signals at δ 58.13 (s, O*C*H_3, a), δ 70.19 (s, O*C*H_2, b), and δ 71.85 (s, O*C*H_2, c).[29]

Mass Transport Properties. Thermal behaviors of the $Mg(hfa)_2 \cdot 2H_2O \cdot 2$diglyme adduct and of the parent $Mg(hfa)_2 \cdot 2H_2O$ complex have been studied by atmospheric pressure thermal gravimetric analysis (TG), differential scanning calorimetry (DSC), and low-pressure TG vaporization rate experiments.

Atmospheric pressure TG analysis of the $Mg(hfa)_2 \cdot 2H_2O \cdot 2$diglyme adduct shows two regions mass loss in the temperature range 40−100 °C and 110−210 °C (Figure 4a). The lower-temperature process, associated with a minor mass loss (∼5%) is well-tuned with the following equation

$$Mg(hfa)_2 \cdot 2H_2O \cdot 2\text{diglyme} \rightarrow Mg(hfa)_2 \cdot 2\text{diglyme} + 2H_2O \quad (2)$$

The remaining 95% mass is lost quantitatively in the second step, almost without residue (<1%) left. Therefore, the lower-temperature process leaves an anhydrous, liquid adduct, which evaporates intact afterward.

Please note that the behavior of the precursor at atmospheric pressure may be different than that occurring during the MOCVD process carried out at 2 Torr. Thus a TG analysis has been carried out at 20 Torr, a pressure that may be considered similar to that occurring during the deposition. At 20 Torr, a single vaporization step has been observed with a significant decrease (about 70 °C) of vaporization temperature with respect to the atmospheric pressure measurement (Figure 4a).

The atmospheric pressure TG curve of the parent $Mg(hfa)_2 \cdot 2H_2O$ presents a two step mass loss (Figure 4a). There is evidence of a dehydration process below 100 °C, and of a sublimation process between 130−260 °C with a low residue left (<5%).

(29) The following notation has been used: diglyme (CH_3-O-CH_2-CH_2)$_2$-O (a, CH_3; b, first CH_2; c, second CH_2).

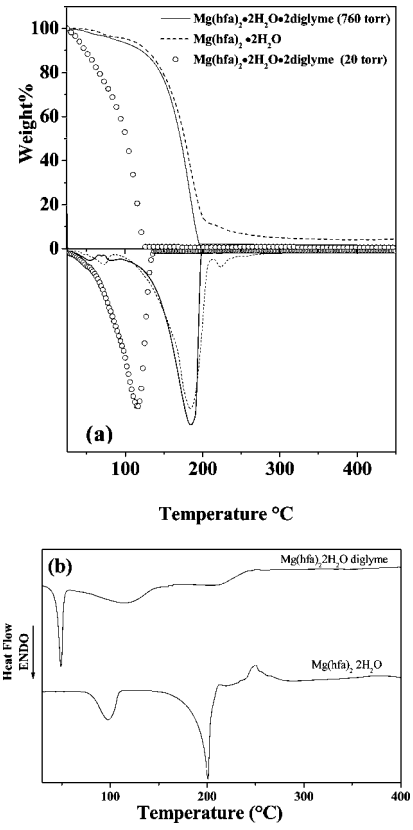

Figure 4. (a) TG-DTG curves of adducts **1**−**2** under N_2 flow in the 25−450 °C temperature range; (b) DSC curves of adducts **1**−**2**.

Figure 4b shows the DSC analyses of the $Mg(hfa)_2 \cdot 2H_2O \cdot 2$diglyme and $Mg(hfa)_2 \cdot 2H_2O$ complexes. In the case of adduct **1**, three distinct endothermic peaks are observed at 48.7, 114, and 205 °C. The sharp endothermic peak is associated with melting of the adduct and matches the melting point observed with the Koeffler microscope. The broad endothermic peaks observed at higher temperatures may be associated with loss of coordinated water and evaporation of the adduct, respectively. Note that the latter is an endothermic peak and therefore the compound evaporates intact without decomposition.

The DSC scan of complex **2** shows three peaks as well (Figure 4b). The lowest broad endothermic peak at around 97.8 °C is associated with water loss. The quite sharp peak at 200.6 °C accounts for melting, whereas the higher temperature peak at 250.2 °C is associated with an exothermic process likely due to partial decomposition overlapping with evaporation.

DSC data indicate that the $Mg(hfa)_2 \cdot 2H_2O \cdot 2$diglyme has better properties with respect to the parent $Mg(hfa)_2 \cdot 2H_2O$ in terms of a much lower melting point and exclusively endothermic processes. It is interesting to note that at difference with other hydrated complexes where H_2O molecules play a key role in determining a multistep decomposition of the adduct;[14f] in the case of $Mg(hfa)_2 \cdot 2H_2O \cdot 2$diglyme, the presence of water does not represent a drawback for the thermal stability of the complex.

Isothermal gravimetric curves of $Mg(hfa)_2 \cdot 2H_2O \cdot 2$diglyme measured in the 60−110 °C range under reduced pressure (20 Torr) and N_2 atmosphere are reported in Figure

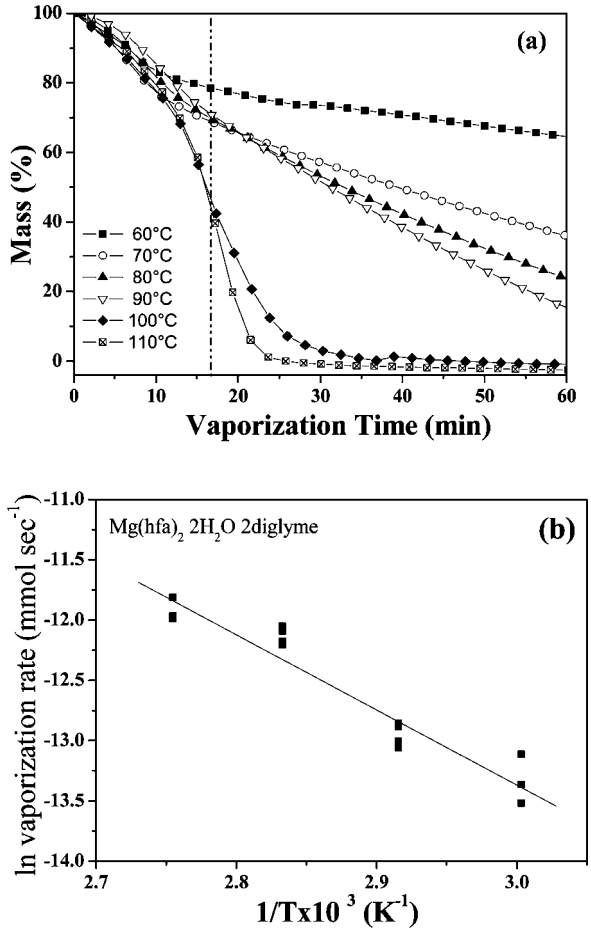

Figure 5. (a) Weight changes with time for vaporization of $Mg(hfa)_2 \cdot 2H_2O \cdot 2$diglyme at various temperatures and reduced pressure of 20 Torr under N_2 flow (the dotted line indicates the longer time needed to reach the settled temperature of 110 °C); (b) Arrhenius plot for the evaporation of $Mg(hfa)_2 \cdot 2H_2O \cdot 2$diglyme.

5a. The curves show a linear behavior in the 60−90 °C range (evaporation from melt) after the settled temperature is reached, as expected for short measurements times.[30] In the 100−110 °C range, a sigmoidal behavior is observed with a too fast evaporation, leading to a complete mass loss after 20−25 min. Nevertheless, an almost linear trend is observed in the intermediate time range. Figure 5b shows the Arrhenius relationship obtained by plotting the ln vaporization rate as a function of the reciprocal temperature in the range 60−90 °C. A linear relationship is evident, as expected for vaporization processes without any side decomposition. The apparent molar enthalpies of the vaporization process (calculated from the slope of the Arrhenius plot) has been evaluated to be 51.8 ± 3.9 kJ mol^{-1}.

Thus adduct **1**, despite the presence of water molecules in the coordination sphere, cleanly self-generates a liquid anhydrous source that represents the first example of a single source of Mg and F elements for MOCVD processes of MgF_2 films.

MOCVD Depositions. The final assessment of a potential precursor for MOCVD processes may be only obtained by applying it to the fabrication of the films of interest. In the present case, the $Mg(hfa)_2 \cdot 2H_2O \cdot 2$diglyme precursor has been validated as a single source through its successful application to the fabrication of MgF_2 films. MgF_2 phase films have been deposited on glass and quartz substrates, under reduced pressure (2 Torr), in the 350−650 °C temperature range. The XRD pattern of the film deposited at 450 °C is reported in Figure 6a. The pattern shows several peaks at $2\theta = 27.30$, 35.25, 40.50, 43.80, 53.60, and 56.35° corresponding to the 110, 101, 111, 210, 211, and 220 reflections, respectively, of the polycrystalline MgF_2 phase.

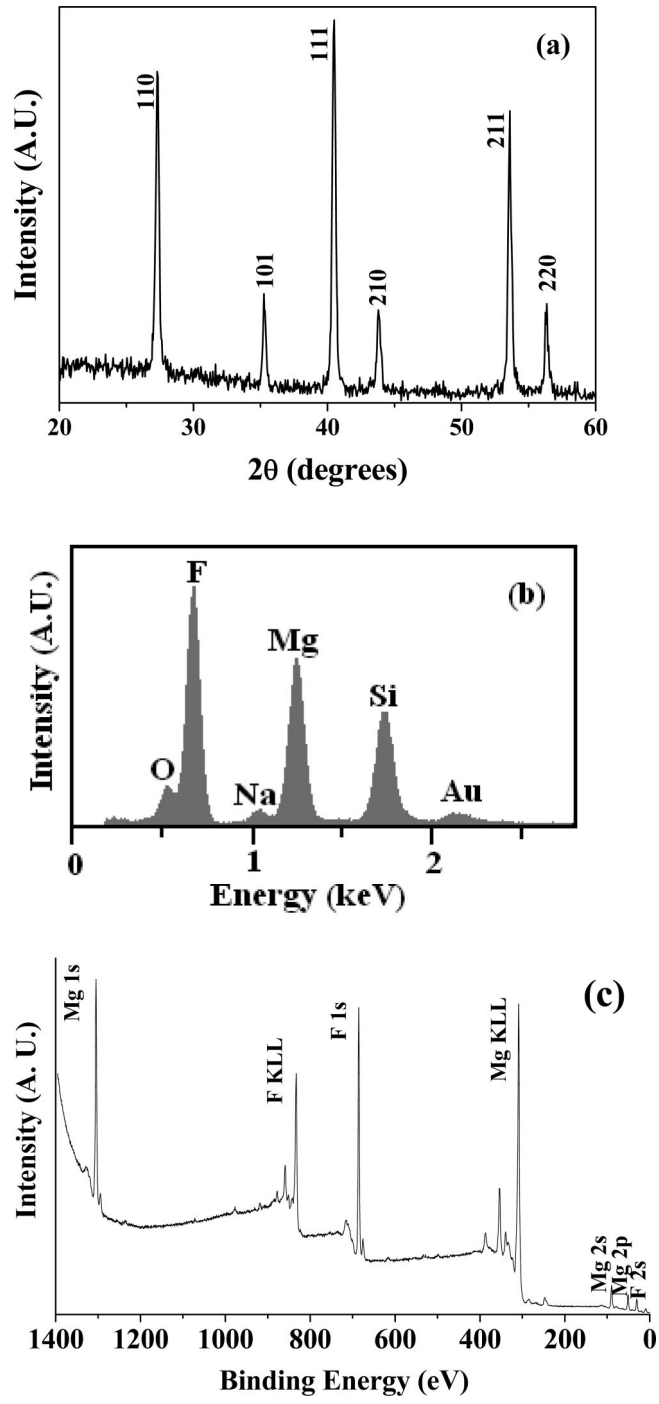

Figure 6. (a) X-ray diffraction pattern of an MOCVD grown MgF_2 film on glass using the $Mg(hfa)_2 \cdot 2H_2O \cdot 2$diglyme as a single source precursor; (b) EDX spectrum of a MgF_2 film deposited on glass; (c) XPS survey spectrum of a MgF_2 film after 30 s sputtering.

(30) Siddiqi, M. A.; Atakan, B. *Thermochim. Acta* **2007**, *452*, 12.

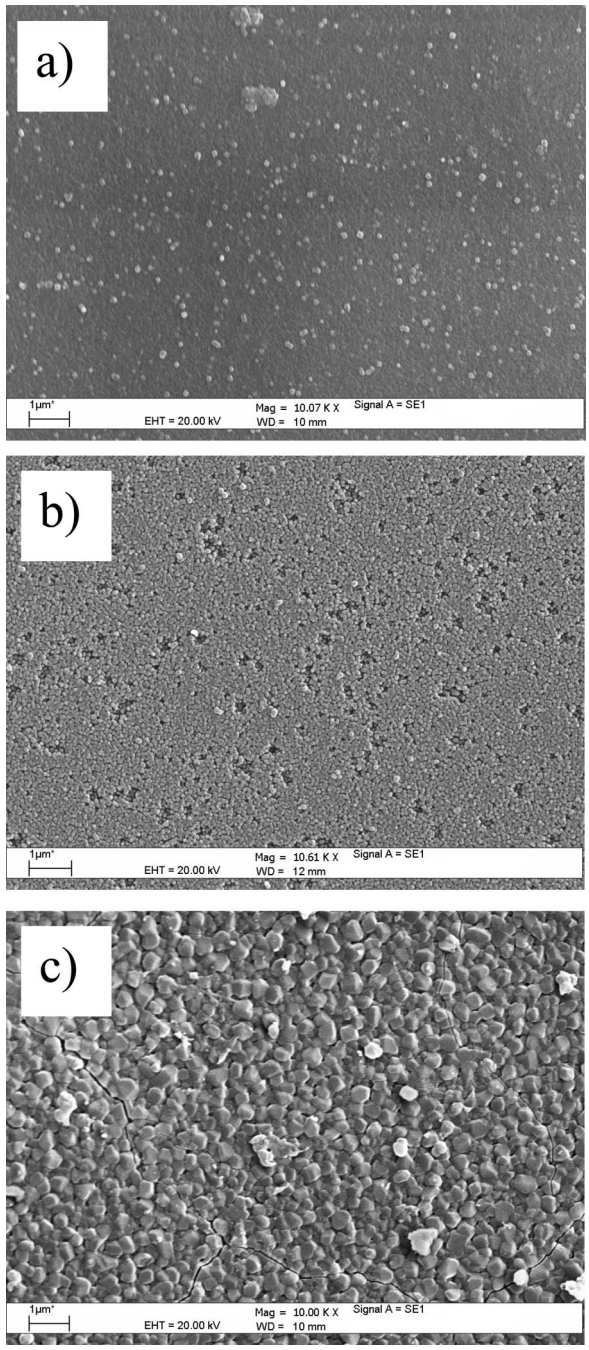

Figure 7. SEM images of MgF_2 films deposited at (a) 350, (b) 450, and (c) 650 °C.

All the peaks, in fact, can be safely associated with reflections of the polycrystalline tetragonal MgF_2 powder (ICDD no. 41−1443).

The compositional purity of the MgF_2 films has been confirmed by energy dispersive X-ray analysis (EDX) and by X-ray photoelectron spectroscopy (XPS). The EDX spectrum, reported in Figure 6b, shows the presence of the Mg Kα peak at about 1.253 KeV. The peak at 1.730 KeV is due to Si Kα peak of the glass substrate, whereas the peak at 2.120 KeV is due to the Au sputtered on the sample. In addition, note that the use of the windowless EDX detector allowed the detection of the F Kα peak at 0.677 KeV and the exclusion of any C contamination. Note that the fluorinating agent is supplied from the source material itself. The O (0.560 KeV) and Na (1.041 KeV) Kα peaks are not contaminants of the films but arise from the glass substrate. The survey XPS spectrum after 30 s sputtering is reported in Figure 6c. It shows the presence of Mg and F. No peaks of O or C have been detected, thus confirming the compositional purity of the MgF_2 phase and excluding the presence of any MgO even as an amorphous phase. The absence of C confirms the clean decomposition of the used precursor.

In regard to morphology, despite the nature of the films remaining the same except for the lowest deposition temperature, the SEM images appear profoundly different. Thus, poorly crystalline phase forms at 350 °C with 100 nm grains (Figure 7a). Very homogeneous smooth surfaces with grains about 200 nm wide are obtained at 450 °C (Figure 7b). Wider crystals about 400 nm wide become evident at 650 °C, giving rise to rougher surface morphologies (Figure 7c). The cracks observed in the films deposited at 650 °C are likely due to the different thermal expansion coefficients between the film and the substrate.

Conclusions

The present one-pot synthetic strategy has proven a very efficient route for the preparation of the novel volatile magnesium adduct from commercially available products. To the best of our knowledge, the adduct $Mg(hfa)_2 \cdot 2H_2O \cdot$ 2diglyme is the first example of a polyglyme magnesium adduct, which represents a single source of Mg and F elements. Thermogravimetric and vaporization rate experiments indicate that it can be used in low-pressure MOCVD depositions at temperatures lower than 100 °C with better thermal behavior than the parent $Mg(hfa)_2 \cdot 2H_2O$, which partially decomposes upon sublimation at significantly higher temperature. In addition, its very low melting point allows its use as a thermally stable precursor in the liquid phase, hence under constant vaporization and mass transport rates.

In summary, this contribution reports the use of an easily synthesized magnesium adduct as a clean single-source Mg/F precursor for the deposition of crystalline MgF_2 thin films under very mild MOCVD conditions. Its vapor phase transport characteristics at low- and atmospheric-pressure make it an attractive candidate not only for laboratory MOCVD processes but also for industrial applications.

Acknowledgment. The authors thank the MIUR for the financial support within the FISR thematic activities: Nanosystems of transition metal oxide for solid oxide fuel cells (SOFCs) (New systems for energy production and storage program). CRIST (Centro Interdipartimentale di Crystallografia Strutturale), University of Florence, is gratefully acknowledged.

Supporting Information Available: Crystallographic information files (CIF). This material is available free of charge via the Internet at http://pubs.acs.org.

CM802923W